

# Ice nucleation of ammonia gas exposed montmorillonite mineral dust particles

A. Salam<sup>1,2</sup>, U. Lohmann<sup>1,3</sup>, and G. Lesins<sup>1</sup>

<sup>1</sup>Department of Physics and Atmospheric Science, Dalhousie University, Halifax, Canada

<sup>2</sup>Department of Chemistry, University of Dhaka, Dhaka – 1000, Bangladesh

<sup>3</sup>Institute of Atmospheric and Climate Science, ETH Zurich, Switzerland

Received: 23 October 2006 – Published in Atmos. Chem. Phys. Discuss.: 10 January 2007

Revised: 10 April 2007 – Accepted: 17 July 2007 – Published: 24 July 2007

**Abstract.** The ice nucleation characteristics of montmorillonite mineral dust aerosols with and without exposure to ammonia gas were measured at different atmospheric temperatures and relative humidities with a continuous flow diffusion chamber. The montmorillonite particles were exposed to pure (100%) and diluted ammonia gas (25 ppm) at room temperature in a stainless steel chamber. There was no significant change in the mineral dust particle size distribution due to the ammonia gas exposure. 100% pure ammonia gas exposure enhanced the ice nucleating fraction of montmorillonite mineral dust particles 3 to 8 times at 90% relative humidity with respect to water (RH<sub>w</sub>) and 5 to 8 times at 100% RH<sub>w</sub> for 120 min exposure time compared to unexposed montmorillonite within our experimental conditions. The percentages of active ice nuclei were 2 to 8 times higher at 90% RH<sub>w</sub> and 2 to 7 times higher at 100% RH<sub>w</sub> in 25 ppm ammonia exposed montmorillonite compared to unexposed montmorillonite. All montmorillonite particles are more efficient as ice nuclei with increasing relative humidities and decreasing temperatures. The activation temperature of montmorillonite exposed to 100% pure ammonia was 15°C higher than for unexposed montmorillonite particles at 90% RH<sub>w</sub>. In the 25 ppm ammonia exposed montmorillonite experiments, the activation temperature was 10°C warmer than unexposed montmorillonite at 90% RH<sub>w</sub>. Degassing does not reverse the ice nucleating ability of ammonia exposed montmorillonite mineral dust particles suggesting that the ammonia is chemically bound to the montmorillonite particle. This is the first experimental evidence that ammonia gas exposed montmorillonite mineral dust particles can enhance its activation as ice nuclei and that the activation can occur at temperatures warmer than –10°C where natural atmospheric ice nuclei are very scarce.

## 1 Introduction

Atmospheric aerosols are important for the direct climate forcing due to their effects on scattering and absorption of solar radiation (Ramaswamy, 2001). Aerosol particles can modify the radiative properties of clouds by acting as cloud condensation nuclei (CCN) and ice nuclei (IN) (Ramanathan et al., 2001; Pruppacher and Klett, 1997; Twomey, 1974). Understanding atmospheric ice formation processes is important in predicting precipitation and cloud radiative properties, both major concerns related to the uncertainties in contemporary climate change (Bailey and Hallett, 2002; Lohmann et al., 2000). Ice particle formation in the atmosphere is usually inefficient since there are relatively few natural ice nuclei especially at temperatures above –20°C (e.g. Schaller and Fukuta, 1979). Heterogeneous ice nucleation involving atmospheric aerosols is the first step in the formation of ice crystals in supercooled liquid water clouds (Hobbs, 1974). This paper presents experimental results where the ice nucleation occurs either in the deposition or condensation freezing mode.

Heterogeneous ice nucleation in the atmosphere with natural dust particles were reported in recent field studies (e.g. Demott et al., 2003; Sassen et al., 2003; Sassen, 2005). Atmospheric dust aerosols can contribute to ice nucleation at large distances from the source (Demott et al., 2003). Laboratory studies have also indicated good ice nucleating properties associated with some types of dust aerosols in the atmosphere (Isono et al., 1959; Field et al., 2006; Kanji and Abbatt, 2006; Knopf and Koop, 2006), especially clay minerals (Zuberi et al., 2002; Roberts and Hallett, 1968) and many of the metal oxide components of dust (Hung et al., 2003). Kanji and Abbatt (2006) studied the ice nucleation of mineral dusts and n-hexane soot particles in the deposition nucleation mode. The deposition mode was found to be efficient for ice formation on mineral dust particles, but not so efficient for the n-hexane soot particles (Kanji and

Correspondence to: A. Salam  
(asalam@mathstat.dal.ca)

Abbatt, 2006). However, montmorillonite is frequently used as a surrogate for atmospheric dust particles in laboratory experiments because it is considered one of the main components of ice nucleating tropospheric mineral dust in the submicron range (Lohmann and Diehl, 2006; Schaller and Fukuta, 1979; Kumai, 1961; Kumai and Francis, 1962). In studies with a continuous flow diffusion chamber of montmorillonite (Salam et al., 2006) and in a large cloud chamber of Sahara, Asian and Arizona test dust (Möhler et al., 2006), it was found that these mineral dust particles act as effective ice nuclei in deposition and condensation nucleation modes.

Chemical and physical interactions can take place between atmospheric trace gases and aerosol particles which may potentially change their ice activation properties (Dymarska et al., 2006; Dontsova et al., 2005; Umann et al., 2005; Russell, 1965). Ammonia is one such trace gas that is produced mainly from anthropogenic sources. In a recent study the interaction of mineral dust particles with gaseous nitric acid, sulfur dioxide and ozone were investigated (Umann et al., 2005). Gaseous nitric acid and ozone were adsorbed on the mineral dust surface, whereas no interaction was observed between sulfur dioxide and mineral dust aerosols (Umann et al., 2005). Knopf and Koop (2006) also studied the heterogeneous ice nucleation behavior of pure and sulfuric acid coated Arizona test dust (ATD) particles. Pure and sulfuric acid coated ATD particles nucleated ice at considerably lower relative humidities than required for homogeneous ice nucleation in liquid aerosols, but no significant difference was observed in the ice nucleation ability between pure and sulfuric acid coated ATD particles (Knopf and Koop, 2006). Dymarska et al. (2006) studied the ice nucleation of soot that was exposed to ozone and found no significant effect of ozone. However, the ice nucleating behavior of mineral dust aerosols due to exposure to ammonia gas has not been studied until now.

In this paper we study the ice nucleation characteristics of ammonia exposed versus non-exposed montmorillonite mineral dust aerosols at temperatures between  $-5^{\circ}\text{C}$  and  $-35^{\circ}\text{C}$  at different relative humidity conditions with the Continuous Flow Diffusion Chamber (CFDC) at Dalhousie University, Canada.

## 2 Experimental methods

### 2.1 Aerosol aging

A stainless steel cylindrical chamber (45 cm long with a diameter of 20 cm) was used to hold the mineral dust particles while being aged in the presence of ammonia gas. About five grams of montmorillonite K10 (Sigma-Aldrich, Powder) mineral dust particles were placed into the bottom of the cylindrical chamber for each aging session. Ammonia gas (100% pure, or 25 ppm diluted in  $\text{N}_2$  gas), with a pressure of 0.5 atmospheres at room temperature was allowed to pass

into the chamber with occasional stirring so that ammonia exposure would be uniform on the dust particles for different exposure times varying from 0 to 2.5 h for 100% ammonia and from 0 to 70 h for 25 ppm ammonia.

### 2.2 Degassing experiment

Ammonia exposed montmorillonite mineral dust particles were degassed at room temperature under a vacuum pressure of  $1.3 \times 10^{-4}$  atmospheres. About 2.0 g of ammonia exposed montmorillonite dust particles were placed in an aluminum container which was placed into a vacuum jar and maintained at vacuum for about 24 h. The degassed montmorillonite was used in FT-IR analyses and also for ice nucleation experiments.

### 2.3 Aerosol surface characteristics

The Fourier transform infrared spectra (FT-IR) using the potassium bromide (KBr) pressed disk technique (e.g. Ogloza and Malhotra, 1989) was conducted using a Bruker FT-IR spectrometer (Model Vector 22). About 1.0 mg mineral dust and 100 mg KBr were weighted and ground in an agate mortar prior to pellet making under a load of  $1.0 \times 10^4$  kg of pressure for 2 min. The pellet was transferred into the sample holder and the FT-IR spectra were measured at room temperature over a wave number range of  $500\text{--}4000\text{ cm}^{-1}$ .

### 2.4 Aerosol generation and impaction

The montmorillonite mineral dust particles were placed into the aerosol generator of the CFDC. The aerosol generator is an airtight reservoir with a vibrating membrane at its base (Salam et al., 2006). The reservoir consists of an aluminum container with a thin, conductive Mylar bottom. The Mylar bottom is held in place with an aluminum collar with an o-ring seal, and is vibrated using a 40 W,  $4\text{g}\Omega$  speaker. The speaker is driven at 5 V using a square wave generator at 1000 Hz. The aerosol particles levitated by the generator were introduced to the flow entering the diffusion chamber. Before entering the chamber the aerosol particles passed through an inertial impactor (Salam et al., 2006; Marple and Willeke, 1976) to remove particles  $>5\ \mu\text{m}$  allowing only montmorillonite mineral dust particles  $\leq 5\ \mu\text{m}$  to enter the CFDC.

### 2.5 Continuous Flow Diffusion Chamber (CFDC) System

The ice nucleation experiments were carried out with the Dalhousie University CFDC (Salam et al., 2006). The CFDC (Fig. 1) is a vertically oriented flow chamber consisting of two concentric circular copper cylinders. The length of the chamber is 161 cm, the top 123 cm is cooled while the bottom 38 cm has no active cooling. The region without cooling

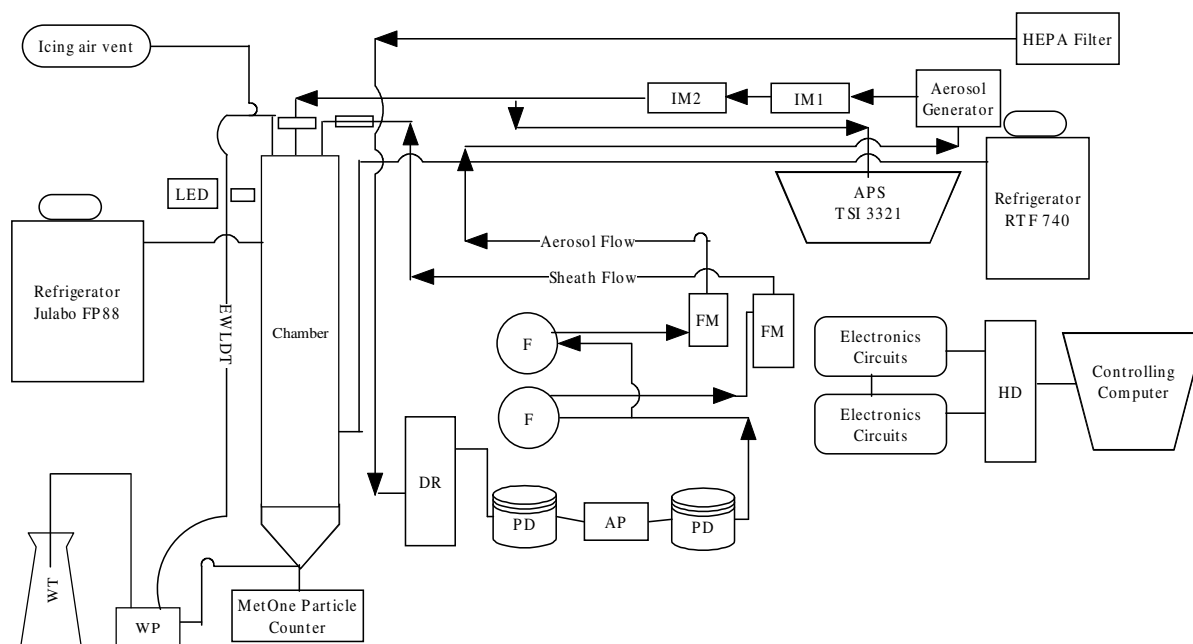


**Fig. 1.** Schematic Diagram of the Continuous Flow Diffusion Chamber (CFDC) at Dalhousie University, Canada. Arrows indicate the airflow in the CFDC system. EWLDT = External Water Level Detection Tube, WT = Water Tank, WP = Water Pump, DR = Drierite holder, F = Inline Filter, FM = Flow Meter, PD = Pulse Dampeners, AP = Air Pump, IM = Impactor, and HD = Computer Hard Disk.

is needed to evaporate any water droplets that might have potentially formed and could be misinterpreted as ice crystals by the particle counter at the exit of the CFDC. The annular gap between the two cylinders, in which the ice crystals grow, is 0.45 cm and this results in a Reynolds Number of about 20, indicative of laminar flow in the annulus gap. Prior to each experiment the annulus gap of the chamber was flooded with water for about 2 s in order to freeze a thin film of ice on the inside walls. During the experiment the two walls are held at two different temperatures at ice saturation which by the diffusion of heat and water vapor creates a steady-state supersaturation with respect to ice near the center of the annulus gap through which the aerosols are carried and, if activated, will grow by water vapor deposition to ice crystals. The air stream containing the aerosols is surrounded by two clean sheath air streams, which confine the aerosols to the center of the annulus gap where the ice supersaturation conditions exist. Typical operating conditions of the chamber are temperatures between  $-2^{\circ}\text{C}$  and  $-45^{\circ}\text{C}$ ; temperature differences between the two walls of  $0^{\circ}\text{C}$  to  $20^{\circ}\text{C}$ ; supersaturation with respect to water (SSw)  $-30\%$  to  $+10\%$ ; supersaturation with respect to ice (SSi)  $0\%$  to  $+50\%$ ; total air flow 2.83 liters per min (lpm) and the residence time for the aerosol particles in the actively cooled portion of the chamber is 20 s. Further details of the CFDC can be found in Salam et al. (2006).

## 2.6 Detection of ice crystals

Aerosol particles  $<5\ \mu\text{m}$  in diameter produced by the aerosol generator were injected into the center of the gap near the location of the maximum supersaturation. Ice crystals were activated, grew in the chamber while being carried by the air stream and were identified with a MetOne (Model 278B) optical particle counter at the outlet of the CFDC (Salam et al., 2006). The flow rate of the MetOne particle counter is 2.83 L/min, which is exactly same as our chamber flow (sum of aerosol flow and two sheath flows). The MetOne particle counter can measure particles with sizes from 0.3 to  $20\ \mu\text{m}$  using 6 size bins (0.3–0.5, 0.5–0.7, 0.7–1, 1–2, 2–5 and 5– $20\ \mu\text{m}$ ). In this study we used the 5– $20\ \mu\text{m}$  size bin for the ice crystal number concentrations measurements. An aerodynamic particle sizer (APS), TSI 3321 was used to verify the accuracy of MetOne particle counter (Model 278B). The total number concentrations of montmorillonite mineral dust particles when measured with both MetOne and APS, agreed within 5% of the number concentration for the same size range. Since the impactor at the input to the CFDC nearly removes all aerosol particles  $>5\ \mu\text{m}$  (a noise level of 0.03% remains as shown below) we can assume, after performing the quality controls described in the next subsection, that all particles  $>5\ \mu\text{m}$  detected by the MetOne are ice crystals. The detected ice nuclei fraction ( $\text{IC}_{>5}/\text{APS}_{<5}$ ) was calculated from the ratio of the total number of ice crystals  $>5\ \mu\text{m}$  detected by the MetOne during the growth experiment ( $\text{IC}_{>5}$ )

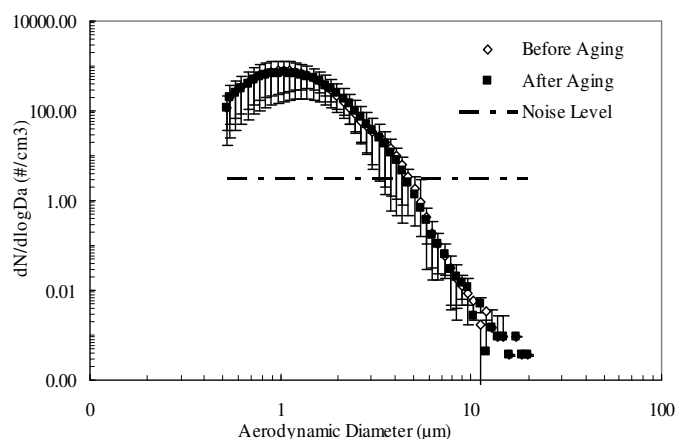


**Fig. 2.** Aerosol particle size distributions of montmorillonite mineral dust before and after aging with ammonia gas as measured with an Aerodynamic Particle Sizer (TSI 3321) exiting the aerosol generation of the CFDC. The dashed line indicates the noise level of the measurements determined from the average number concentrations of blank (no montmorillonite particle input into the chamber flow) and dry (montmorillonite particle input in the chamber flow but no ice coating on the chamber walls) experiments. The vertical bars are the error bars equal to the standard deviation of the 20 samples (duration of each sample is 60 s).

to the average of the total number of aerosol particles  $<5 \mu\text{m}$  ( $\text{APS}_{<5}$ ) measured before and after each ice nucleation experiment.

### 2.7 Quality control of the CFDC measurements

All experiments used filtered and dried air for both the sheath and aerosol flows. An ULPA air filter preceded by a HEPA air filter removed 99.97% of the ambient aerosols  $>0.1 \mu\text{m}$ . The air streams were dried down to a dew point of  $-73^\circ\text{C}$  with anhydrous calcium sulfate Drierite (W. A. Hammond Drierite Co). To check the presence of any ice particle artifacts both blank and dry experiments were conducted. In a blank experiment no aerosol particles are input into the chamber flow but the chamber walls are coated with ice. In a dry experiment aerosol particles are input into the chamber but there is no ice coating on the chamber walls. Before running any blank experiment we passed dried and filtered air into the CFDC for about eight hours to remove all particles that may have remained inside the system from the previous experiment.

We used the total aerosol particle number concentrations  $<5 \mu\text{m}$  ( $\text{APS}_{<5}$ ) before and after the ice nucleation experiments in the calculation of the percentage of ice activation because it was not possible to measure the input aerosol number concentrations during the actual ice nucleation experiment. This is not a problem because of the high reproducibility ( $\pm 5\%$ ) that was obtainable for the input aerosol number concentration. Moreover, we are unable to differentiate be-

tween aerosol and ice particles below  $5 \mu\text{m}$  and so we had to use particles greater than  $5 \mu\text{m}$  as the criterion for ice particles. Hence we are unable to report the total ice nucleation rate, but rather report the ice nucleation percentage based on the ratio of ice crystals that grew to sizes beyond  $5 \mu\text{m}$  to the pre-nucleation particle concentration.

To rule out the possibility of hygroscopic growth by the aerosol particles within the CFDC it was checked whether montmorillonite adsorbed enough water vapor to grow  $>5 \mu\text{m}$ . The test was done by setting the temperature of both ice-covered walls of the chamber to  $-2^\circ\text{C}$ . The relatively warm temperature of  $-2^\circ\text{C}$  was chosen to get very close to water saturation conditions (98.1% RHw) in the chamber. The detected ice crystal fraction ( $\text{IC}_{>5}/\text{APS}_{<5}$ ) was only 0.04% at the outlet of the chamber, which is within the noise level as determined by the blank as well as the dry experiments. Blank experiments were carried out with no montmorillonite aerosol particles input into the chamber. Dry experiments were carried out with montmorillonite aerosol particles passing through the CFDC flows but there was no ice coating on the chamber walls. We also carried out ice nucleation experiments using water vapor instead of ammonia to age the montmorillonite dust aerosols. The percentage of the detected ice nuclei of montmorillonite dust aerosols due to the exposure to water vapor for 24 h instead of ammonia gas was 1.02% at 90% RHw at  $-30^\circ\text{C}$ . However, the percentages of detected ice nuclei of water vapor exposed montmorillonite were similar to that of the pure montmorillonite, which indicates that water vapor exposure alone has no significant effect on the ice nucleation ability of the montmorillonite dust aerosol particles.

## 3 Results and discussion

### 3.1 Aerosol size distributions

The initial size distributions of the mineral dust aerosol particles before injection into the CFDC were determined with an aerodynamic particle sizer (APS), Model TSI 3321 (Peters and Leith, 2003) both with and without ammonia exposure (Fig. 2). The TSI APS is widely used for aerosol measurements and provides accurate size distributions (Peters and Leith, 2003). The size range of the APS is from  $0.5$  to  $20 \mu\text{m}$  in diameter. The resolution of the APS is  $0.02 \mu\text{m}$  at  $1.0 \mu\text{m}$  diameter and  $0.03 \mu\text{m}$  at  $10 \mu\text{m}$  diameter. The particles size distributions were measured after the impactor system with a size cut off of  $5 \mu\text{m}$ . Due to the fixed design of the impactor, it is not possible to measure the size distribution before and after the impactor. However, the size distribution curve shows the variation of aerodynamic diameter versus number concentration ( $\text{dN}/\text{dlog}D_a$ ) between  $0.5$  and  $20 \mu\text{m}$  (Fig. 2). The total number concentration of aerosol particles  $<5 \mu\text{m}$  in diameter that are input into the CFDC is almost the same (about  $1.05 \times 10^4 \text{ cm}^{-3}$ ) for both ammonia-exposed

and non-exposed montmorillonite. Only 0.03% of all particles ( $3.2 \text{ cm}^{-3}$ ) were found to be  $>5 \mu\text{m}$ , which is below the noise level as shown in Fig. 2. The noise level was determined from particle artifacts measured during the blank and dry experiments described in Sect. 2.7.

### 3.2 Fourier Transform Infrared (FT-IR) analysis

The spectra of montmorillonite, ammonia exposed montmorillonite and degassed (after ammonia exposure) montmorillonite mineral dust particles at room temperature are given in Fig. 3. The FT-IR spectrum of pure montmorillonite is shown in Fig. 3a. It shows the typical absorption bands of montmorillonite (Farmer, 1974), for example Al-OH-Al (Ogloza and Malhotra, 1989) stretching at  $3625 \text{ cm}^{-1}$ , OH (Ogloza and Malhotra, 1989; Russell, 1965) stretching of water at  $3434 \text{ cm}^{-1}$  and Si-O (Ogloza and Malhotra, 1989; Russell, 1965) bending at  $1059 \text{ cm}^{-1}$ . However, there is a broad peak at the band position of about  $3220 \text{ cm}^{-1}$  in Figs. 3b and 3c, which is very weak for pure montmorillonite (Fig. 3a). Hydroxyl and amino groups show characteristic absorption bands (Coates, 2000; Ogloza and Malhotra, 1989) in the region from  $3650$  to  $3200 \text{ cm}^{-1}$ . Therefore the weak peak at  $3220 \text{ cm}^{-1}$  in the case of pure montmorillonite (Fig. 3a) is most likely an extended peak of the hydroxyl groups. In Figs. 3b and 3c, the N-H stretching of the ammonia molecule result in a more pronounced peak at  $3220 \text{ cm}^{-1}$ . There is another small IR signature peak for ammonium at around  $1400 \text{ cm}^{-1}$  in Figs. 3b and 3c, which is also less dominant in Fig. 3a. Thus, the similarity of the peak positions between ammonia exposed and degassed montmorillonite mineral dust indicates the retention of ammonia into the montmorillonite interlayer space and/or that ammonia is adsorbed chemically (Russell, 1965).

### 3.3 Ice nucleation experiments with varying exposure times

Ice nucleation experiments of aged montmorillonite dust particles were performed by varying the ammonia gas exposure times from 0 to 2.5 h for 100% pure ammonia (Fig. 4 top), and 0 to 70 h for 25 ppm ammonia (Fig. 4 bottom) before injecting them into the CFDC at 100% and 90% relative humidities at a temperature of  $-20^\circ\text{C}$ . About 0.7% of the 100% pure ammonia aged montmorillonite particles were detected as ice nuclei at 90% RHw, and 2.7% at 100% RHw with only one min of ammonia gas exposure. In contrast, only about 0.4% and 0.7% of the non-aged montmorillonite particles were detected as ice nuclei at 90% RHw and 100% RHw, respectively (Fig. 4 top). The percentage of detected aged montmorillonite as ice nuclei increases with the exposure times up to 2 h and then reaches a saturation level at about 1.5% at 90% RHw and at about 7.8% at 100% RHw (Fig. 4 top). In the case of 25 ppm ammonia exposed montmorillonite (Fig. 4 bottom), the detected ice nuclei (%) frac-

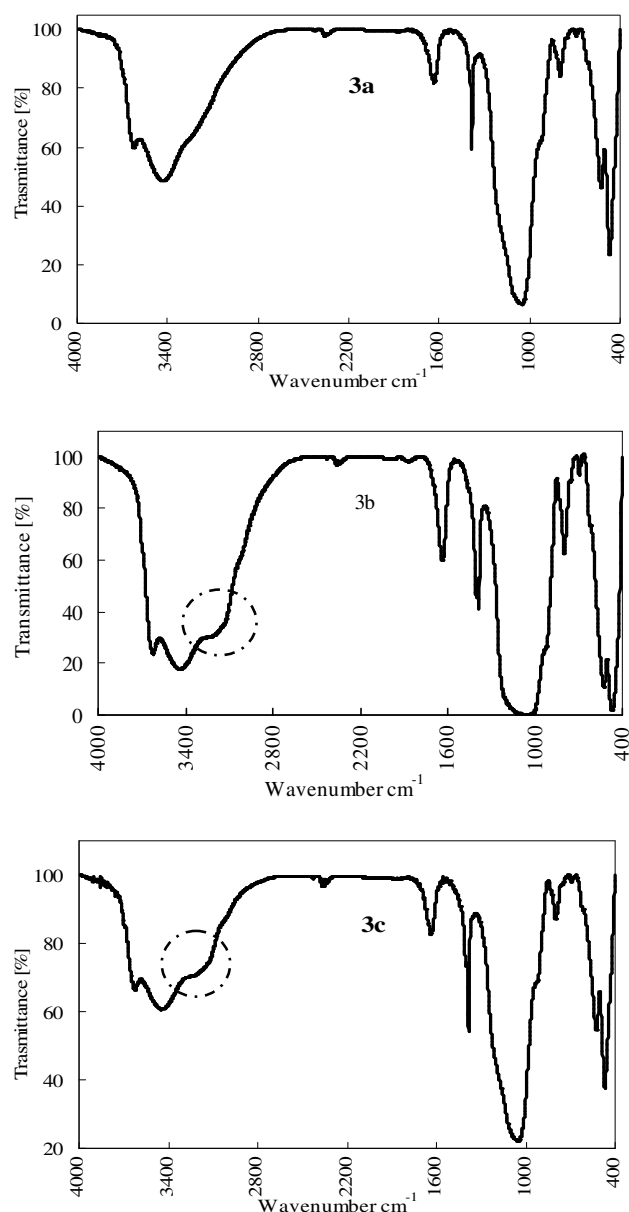


**Fig. 3.** The Fourier transform infrared (FT-IR) spectra of pure montmorillonite 3a, ammonia exposed montmorillonite 3b, degassed (after ammonia exposure) montmorillonite 3c with Bruker FTIR instruments, Model Vector 22. The absorption band at  $3220 \text{ cm}^{-1}$  suggests chemi-adsorbed ammonia indicated by the dashed circle in Figs. 3b and 3c.

tion increases below 20 h exposure time and then attains a saturation level with increasing exposure times. The higher fractions of activation in the case of aged montmorillonite at 100% RHw in Fig. 4 are caused by either condensation freezing or enhanced deposition nucleation. It should be pointed out that our percentages of ice activation may be underestimated since we are unable to detect ice crystals  $<5 \mu\text{m}$  exiting the CFDC.

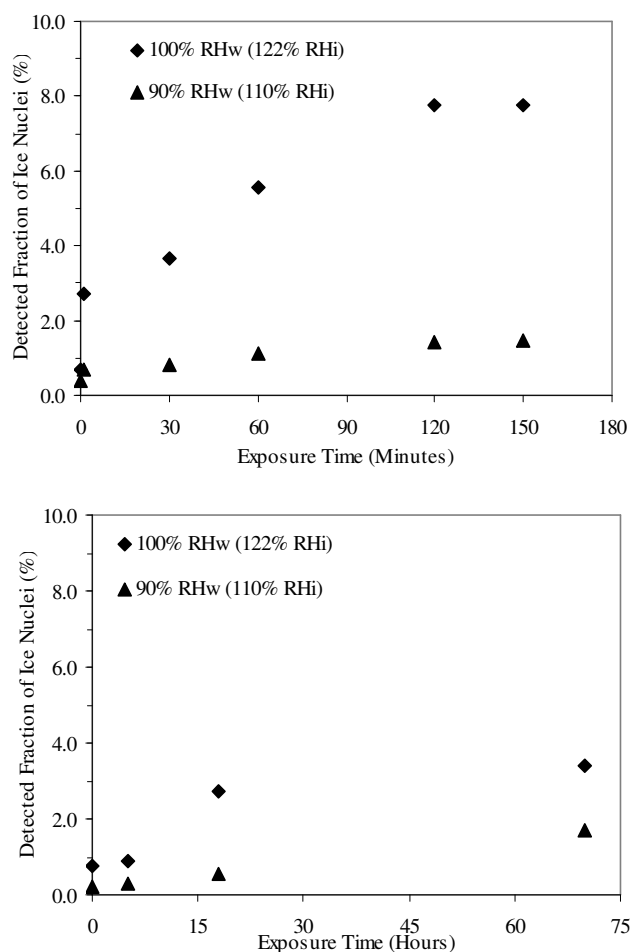


**Fig. 4.** Percentage of detected fraction of ice nuclei versus 100% pure (top) and 25 ppm (bottom) ammonia gas exposure time of montmorillonite mineral dust particles at 100% and 90% relative humidity with respect to water (RHw) (corresponding relative humidities with respect to ice are 110% and 122%, respectively) at  $-20^{\circ}\text{C}$ . The percentage of detected fraction of ice nuclei ( $\text{IC}_{>5}/\text{APS}_{<5}$ ) was calculated from the ratio of the total number of ice crystals  $>5\ \mu\text{m}$  ( $\text{IC}_{>5}$ ) to the average of the total number of aerosol particles  $<5\ \mu\text{m}$  ( $\text{APS}_{<5}$ ) before and after of each ice nucleation experiments. Results at 0 min exposure time stem from the non-aged experiments.

### 3.4 Ice nucleation experiments with varying temperatures

#### 3.4.1 With 100% pure ammonia gas

In this series of experiments the 100% pure ammonia exposure time was fixed at 2 h at each temperature. The air temperature was varied between  $-5^{\circ}\text{C}$  and  $-35^{\circ}\text{C}$  at 90 to 100% RHw in  $5^{\circ}\text{C}$  temperature intervals. There was a set of 15 experiments at each temperature including blank and dry experiments. The detected ice nuclei fraction ( $\text{IC}_{>5}/\text{APS}_{<5}$ ), expressed as a percentage, versus temperature for montmorillonite mineral dust aerosols with and without exposure to

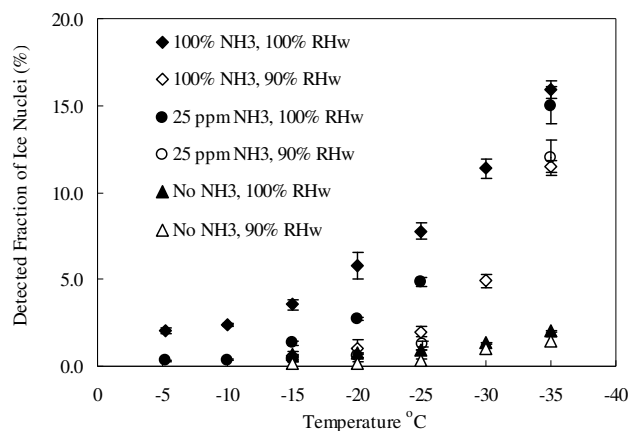


**Fig. 5.** Percentage of detected fraction of ice nuclei (as defined in Fig. 4) versus temperature ( $^{\circ}\text{C}$ ) of montmorillonite mineral dust particle exposed to 100% pure or 25 ppm ammonia gas and without ammonia gas exposure at 90% and 100% relative humidity with respect to water (RHw) (corresponding relative humidities with respect to ice have given in Table 1). The exposure time was 2 h for 100% pure ammonia and 18 h for 25 ppm ammonia. The vertical bars are the error bars equal to the standard deviation of the 15 measurements conducted at each temperature.

ammonia gas at 90% and 100% RHw is shown in Fig. 5. The fraction of montmorillonite dust particles that act as ice nuclei increased 3 to 8 times due to exposure to 100% ammonia gas at 90% RHw, and 5 to 8 times at 100% RHw within the temperature range of  $-15^{\circ}\text{C}$  and  $-35^{\circ}\text{C}$  (Table 1). All montmorillonite aerosol particles are more efficient as ice nuclei with increasing relative humidities and decreasing temperatures (Fig. 5).

The activation temperature is defined as the warmest temperature at which the detected fraction of ice crystals  $>5\ \mu\text{m}$  is at least 1% of the average of the total number of montmorillonite aerosol particles  $<5\ \mu\text{m}$  before and after each ice nucleation experiment. This activation temperature criterion is tightly related to our experimental setup and care should be exercised when comparing it with other studies. However, ice nucleation activity was observed at a temperature of  $-5^{\circ}\text{C}$  and  $-15^{\circ}\text{C}$  for the 100% ammonia aged montmorillonite mineral dust at 100% and 90% RHw, respectively (Table 2), whereas the ice nucleation activity for pure montmorillonite mineral dust aerosol particles was observed at temperatures of  $-20^{\circ}\text{C}$  at 100% RHw and of  $-30^{\circ}\text{C}$  at 90% RHw (Table 2). This is a significant finding since natural ice nuclei that are active at temperatures warmer than  $-10^{\circ}\text{C}$  are very scarce (e.g. Schaller and Fukuta, 1979). This is the first experimental evidence that ammonia gas exposure to montmorillonite mineral dust particles can raise the heterogeneous ice nucleation activation temperature to warmer than  $-10^{\circ}\text{C}$ .

**Table 1.** Enhancement of ice nucleation due to the exposure of montmorillonite mineral dust particles to 100% pure and 25 ppm ammonia at 90% and 100% relative humidity with respect water (RHw) at different temperatures. Equations  $e_s(T) = 611.21 (273.15/T)^{5.0206} \exp(6790.66 (1/273.15 - 1/T))$  and  $e_i(T) = 611.21 \exp(L_s/R_v (1/273.15 - 1/T))$  were used for the calculation of saturation vapor pressure with respect to water ( $e_s$ ) and ice ( $e_i$ ). These two equations were derived from the Clausius-Clapeyron equation (Rogers and Yau, 1989). Where,  $e_s$  is the saturation vapor pressure with respect to water,  $T$  is the temperature,  $e_i$  is the saturation vapor pressure with respect to ice,  $L_s$  is the latent heat of sublimation, and  $R_v$  is the gas constant for water vapor. We compared the above two equations with the values of  $e_s$  (Waxler, 1976) and  $e_i$  (Waxler, 1977) in Table 2.1. of Rogers and Yau (1989) and found a maximum deviation of about 0.2% between  $-40^\circ\text{C}$  and  $0^\circ\text{C}$ .

Temperature ( $^\circ\text{C}$ )	Corresponding relative humidity with respect to ice (RH <sub>i</sub> ) in percentage (%)		Enhancement factor for ice nucleation (aged montmorillonite/ non aged montmorillonite)			
	For		100% pure ammonia		25 ppm ammonia	
	100% RHw	90% RHw	100% RHw	90% RHw	100% RHw	90% RHw
-15	116	104	5	3	2	2
-20	122	110	8	5	4	3
-25	128	115	8	6	5	4
-30	136	121	8	5	–	–
-35	143	127	8	8	7	8

### 3.4.2 With 25 ppm diluted ammonia gas

Ice nucleation experiments of montmorillonite mineral dust particles were also carried out with 25 ppm ammonia gas at temperatures between  $-5^\circ\text{C}$  and  $-35^\circ\text{C}$  at 90% and 100% RHw with an 18 h exposure time (Fig. 5). The concentration of the diluted ammonia used in these series of experiments is still significantly higher than the concentration of atmospheric ammonia in polluted regions (e.g. Godish, 2003). Our experimental setup prevented further dilution of the gas. However the effect of the ammonia gas on ice nucleation will also be determined by the exposure time which can be longer in the atmosphere and help to compensate for the lower concentrations found in the real atmosphere. The fraction of montmorillonite dust particles detected as ice nuclei increased 2 to 7 times at 100% RHw and 2 to 8 times at 90% RHw due to the modification of the montmorillonite dust surface by 25 ppm ammonia from temperatures of  $-15^\circ\text{C}$  to  $-35^\circ\text{C}$  (Table 1). Our study shows enhanced ice nucleation of montmorillonite dust particles aged with 25 ppm ammonia gas exposure, which is 3 orders of magnitude  $>$  found in highly polluted situations (e.g. Godish, 2003).

The activation temperature of 25 ppm ammonia exposed montmorillonite mineral dust aerosols was  $-15^\circ\text{C}$  at 100% RHw (Table 2); whereas the activation temperature of unexposed montmorillonite was  $-20^\circ\text{C}$  at 100% RHw (Table 2). The activation temperature of 25 ppm ammonia exposed montmorillonite was  $10^\circ\text{C}$  warmer than non exposed montmorillonite at 90% RHw (Table 2).

Some possible mechanisms for the ammonia adsorption or retention on the montmorillonite surface include coordination of ammonia to the exchangeable cations, formation of ammonium cations, hydrogen bonding of  $\text{NH}_3$  to the montmorillonite surface and trapping of  $\text{NH}_3$  molecules in the

**Table 2.** The activation temperature of pure (100%) ammonia exposed montmorillonite, 25 ppm ammonia exposed montmorillonite, and non-exposed (pure) montmorillonite mineral dust particles at 100% and 90% relative humidity with respect to water (RHw).

Montmorillonite mineral dust aerosol particles	Activation temperature ( $^\circ\text{C}$ ) at	
	100% RHw	90% RHw
100% ammonia exposed	-5	-15
25 ppm ammonia exposed	-15	-20
Non exposed (pure)	-20	-30

interlayer space (e.g. Dontsova et al., 2005; Russell, 1965; Mortland et al., 1963). A likely scenario is that ammonia molecules replace water in the interlayer space of montmorillonite in an atmosphere of ammonia (Russell, 1965). In the current study the FT-IR measurements suggest that the ammonia is chemically adsorbed in the montmorillonite. It is possible that the addition of ammonia enables liquid water uptake so that ammonia-aged montmorillonite mineral dust aerosols are activated in condensation freezing mode first, and followed by deposition mode, which enhanced the heterogeneous ice nucleation ability of ammonia gas exposed montmorillonite mineral dust aerosol particles.

### 3.5 Ice nucleation experiments using degassed montmorillonite

The ice nucleation experiments using degassed montmorillonite (after 100% ammonia exposure for 24 h) were carried out in the CFDC system and compared to 100% ammonia exposed montmorillonite for the same duration without degassing. The experimental conditions for this comparison

were at  $-30^{\circ}\text{C}$  and 90% RHw. Enhanced ice nucleation was observed in both non-degassed and degassed ammonia exposed montmorillonite mineral dust aerosols with a detected fraction of ice nuclei of 4.9% in the 100% ammonia exposed and a detected fraction of ice nuclei of 4.89% in the degassed experiment. This result indicates that degassing does not reverse the ice nucleating ability of ammonia exposed montmorillonite. This is expected if the ammonia molecules are chemically adsorbed into the montmorillonite as suggested by the FT-IR spectra.

#### 4 Conclusions

The importance of ammonia on the aging of montmorillonite mineral dust particles for ice nucleation was studied for different exposure times, air temperatures and relative humidity conditions with the Dalhousie University Continuous Flow Diffusion Chamber. The ice nucleation increases with increasing ammonia gas exposure time and relative humidity. Only 1.5% of the 100% pure ammonia aged montmorillonite particles were detected as ice nuclei that eventually grew to a size  $>5\ \mu\text{m}$  at 90% RHw at  $-20^{\circ}\text{C}$ . The detected ice nucleating fraction of montmorillonite dust particles increased 3 to 8 times at 90% RHw due to the exposure to 100% ammonia and 2 to 8 times at 90% RHw due to the exposure to 25 ppm ammonia compared to non exposed particles. The activation temperature of 100% pure ammonia aged montmorillonite mineral dust particles was found to be  $15^{\circ}\text{C}$  warmer than that of the non-aged montmorillonite at both 100% and 90% RHw. The activation temperature of 25 ppm ammonia exposed montmorillonite mineral dust aerosols was  $-15^{\circ}\text{C}$  at 100% RHw, which is  $5^{\circ}\text{C}$  warmer than non exposed pure montmorillonite. Ammonia exposed and then degassed montmorillonite dust aerosols have similar ice nucleation efficiencies. This along with the infrared transmission spectra suggests that the ammonia is chemi-adsorbed in the montmorillonite.

This is the first experimental evidence for an enhancement of ice nucleation by mineral dust aerosols exposed to ammonia gas. Although the ammonia concentrations used are higher than those found in the polluted atmosphere the effect has been demonstrated and future experiments will be performed using lower concentrations. Not only was there an increase in the activated fraction of montmorillonite aerosols for the temperatures and relative humidities used in this study, but the aged aerosols were able to initiate ice nucleation at temperatures warmer than  $-10^{\circ}\text{C}$  where very few natural ice nuclei are found. This is potentially an important way that anthropogenic trace gases can change the atmospheric cloud properties and precipitation development by the ice particle phase with significant climate change implications.

*Acknowledgements.* We are grateful for support from the Canadian Foundation for Climate and Atmospheric Sciences (CFCAS) and

the National Science and Engineering Research Council (NSERC) of Canada. We thank B. Crenna for his excellent work in constructing and testing the CFDC. We also acknowledge H. Phillips and A. Dyker for helping with the FT-IR, and K. Borgel and A. George for their technical help.

Edited by: T. Koop

#### References

- Bailey, M. and Hallett, J.: Nucleation effects on the habit of vapour grown ice crystals from  $-18$  to  $-42^{\circ}\text{C}$ , *Q. J. Roy. Meteor. Soc.*, 128, 1461–1483, 2002.
- Coates, J.: *Encyclopedia of Analytical Chemistry*, edited by: Meyers, R. A., Chichester, 10815, 2000.
- DeMott, P. J., Sassen, K., Poellot, M. R., Baumgardner, D., Rogers, D. C., Brooks, S. D., Prenni, A. J., and Kreidenweis, S. M.: African dust aerosols as atmospheric ice nuclei, *Geophys. Res. Lett.*, 30(14), 1732, doi:10.1029/2003GL017410, 2003.
- Dontsova, K. M., Norton, L. D., and Johnston, C. T.: Calcium and Magnesium Effects on Ammonia Adsorption by Soil Clays, *Soil Sci. Soc. Am. J.*, 69, 1225–1232, 2005.
- Dymarska, M., Murray, B. J., Sun, L., Eastwood, M. L., Knopf, D. A., and Bertram, A. K.: Deposition ice nucleation on soot at temperatures relevant for the lower troposphere, *J. Geophys. Res.*, 111, D04204, doi:10.1029/2005JD006627, 2006.
- Farmer, V. C.: *The infrared spectra of minerals*, Mineralogical Soc, London, 331, 1974.
- Field, P. R., Möhler, O., Connolly, P., Krämer, M., Cotton, R., Heymsfield, A. J., Saathoff, H., and Schnaiter, M.: Some ice nucleation characteristics of Asian and Saharan desert dust, *Atmos. Chem. Phys.*, 6, 2991–3006, 2006, <http://www.atmos-chem-phys.net/6/2991/2006/>.
- Godish, T.: *Air Quality*, 4th Edition, Lewis Publishers, 42, 2003.
- Hobbs, P. V.: *Ice Physics*, Oxford University Press, Oxford, 837, 1974.
- Hung, H.-M., Malinowski, A., and Martin, S. T.: Kinetics of heterogeneous ice nucleation on the surfaces of mineral dust cores inserted into aqueous ammonium sulfate particles, *J. Phys. Chem. A*, 107, 1296–1306, 2003.
- Isono, K., Komabayasi, M., and Ono, A.: The nature and origin of ice nuclei in the atmosphere, *J. Meteor. Soc. Japan.*, 37, 211–233, 1959.
- Kanji, Z. A. and Abbatt, J. P. D.: Laboratory studies of ice formation via deposition mode nucleation onto mineral dust and n-hexane soot samples, *J. Geophys. Res.*, 111, D16204, doi:10.1029/2005JD006766, 2006.
- Knopf, D. A. and Koop, T.: Heterogeneous nucleation of ice on surrogates of mineral dust, *J. Geophys. Res.*, 111, D12201, doi:10.1029/2005JD006894, 2006.
- Kumai, M.: Snow crystals and the identification of the nuclei in the northern United States of America, *J. Meteorol.*, 18, 139–150, 1961.
- Kumai, M. and Francis, K. E.: Nuclei in snow and ice crystals on the Greenland ice cap under natural and artificially stimulated conditions, *J. Atmos. Sci.*, 19, 474–481, 1962.
- Lohmann, U., Feichter, J., Penner, J. E., and Leaitch, R.: Indirect effect of sulfate and carbonaceous aerosols: A mechanistic treatment, *J. Geophys. Res.*, 105, 12 193–12 206, 2000.

- Lohmann, U. and Diehl, K.: Sensitivity studies of the importance of dust ice nuclei for the indirect aerosol effect on stratiform mixed-phase clouds, *J. Atmos. Sci.*, 63, 968–982, 2006.
- Marple, V. A. and Willeke, K.: Impactor Design, *Atmos. Environ.*, 10, 891–896, 1976.
- Mortland, M. M., Fripiat, J. J., Chaussidon, J., and Uytterhoeven, J.: Interaction between ammonia and the expanding lattices of montmorillonite and vermiculite, *J. Phys. Chem.*, 67, 248–258, 1963.
- Möhler, O., Field, P. R., Connolly, P., Benz, S., Saathoff, H., Schnaiter, M., Wagner, R., Cotton, R., Krämer, M., Mangold, A., and Heymsfield, A. J.: Efficiency of the deposition mode ice nucleation on mineral dust particles, *Atmos. Chem. Phys.*, 6, 3007–3021, 2006, <http://www.atmos-chem-phys.net/6/3007/2006/>.
- Ogloza, A. A. and Malhotra, V. M.: Dehydroxylation Induced Structural Transformations in Montmorillonite: an Isothermal FTIR Study, *Phys. Chem. Minerals*, 16, 378–385, 1989.
- Peters, T. M. and Leith, D.: Concentration measurement and counting efficiency of the aerodynamic particle sizer 3321, *J. Aero. Sci.*, 34(5), 627–634, 2003.
- Pruppacher, H. R. and Klett, J. D.: *Microphysics of Clouds and Precipitation*, Kluwer Academic, Norwell, Mass, 954, 1997.
- Ramanathan, V., Crutzen, P. J., Kiehl, J. T., and Rosenfeld, D.: Aerosols, climate, and the hydrological cycle, *Science*, 294, 2119–2124, 2001.
- Ramaswamy, V.: Radiative forcing of climate change, in *Climate Change 2001, The Scientific Basis*, Cambridge Univ. Press, New York, 349–406, 2001.
- Roberts, P. and Hallett, J.: A laboratory study of the ice nucleating properties of some mineral particulates, *Q. J. Roy. Meteor. Soc.*, 94, 25–34, 1968.
- Rogers, R. R. and Yau, M. K.: *A Short Course in Cloud Physics*, Pergamon Press, NY, 12–17, 1989.
- Russell, J. D.: Infra-red Study of the Reactions of Ammonia with montmorillonite and Saponite, *Trans. Faraday Soc.*, 61, 2284–2294, 1965.
- Salam, A., Lohmann, U., Crenna, B., Lesins, G., Klages, P., Rogers, D., Irani, R., MacGillivray, A., and Coffin, M.: Ice Nucleation Studies of Mineral Dust Particles with a New Continuous Flow Diffusion Chamber, *Aero. Sci. Tech.*, 40(2), 134–143, 2006.
- Sassen, K., DeMott, P. J., Prospero, J. M., and Poellot, M. R.: Saharan dust storms and indirect aerosol effects on clouds: CRYSTAL-FACE results, *Geophys. Res. Lett.*, 30(12), 1633, doi:10.1029/2003GL017371, 2003.
- Sassen, K.: Dusty ice clouds over Alaska, *Nature*, 434 (7032), 456–456, 2005.
- Schaller, R. C. and Fukuta, N.: Ice nucleation by aerosol particles: Experimental studies using a wedge-shaped ice thermal diffusion chamber, *J. Atmos. Sci.*, 36, 1788–1802, 1979.
- Twomey, S.: Pollution and planetary albedo, *Atmos. Environ.*, 8(12), 1251–1256, 1974.
- Umann, B., Arnold, F., Schaal, C., Hanke, M., Uecker, J., Aufmhoff, H., Balkanski, Y., and Van Dingenen, R.: Interaction of mineral dust with gas phase nitric acid and sulfur dioxide during the MINATROC II field campaign: First estimate of the uptake coefficient  $\gamma_{\text{HNO}_3}$  from atmospheric data, *J. Geophys. Res.*, 110, D22306, doi:10.1029/2005JD005906, 2005.
- Wexler, A.: Vapor pressure formulation for water in the range 0 to 100°C. A revision, *J. Res. Nat. Bur. Stand.*, 80A, 775–785, 1976.
- Wexler, A.: Vapor pressure formulation for ice, *J. Res. Nat. Bur. Stand.*, 81A, 5–20, 1977.
- Zuberi, B., Bertram, A. K., Cassa, C. A., Molina, L. T., and Molina, M. J.: Heterogeneous nucleation of ice in  $(\text{NH}_4)_2\text{SO}_4\text{-H}_2\text{O}$  particles with mineral dust immersions, *Geophys. Res. Lett.*, 29(10), 1504, doi:10.1029/2001GL014289, 2002.